Transverse quark spin effects and the flavor dependence of the Boer-Mulders function

Leonard P. Gamberg,[1] Gary R. Goldstein,[2] and Marc Schlegel[3]
[1]*Division of Science, Penn State Berks, Reading, Pennsylvania 19610, USA*
[2]*Department of Physics and Astronomy, Tufts University, Medford, Massachusetts 02155, USA*
[3]*Theory Center, Jefferson Lab, Newport News, Virginia 23608, USA*
(Received 1 October 2007; published 21 May 2008)

The naive time-reversal-odd (''T-odd'') parton distribution $h_1^\perp$, the so-called Boer-Mulders function, for both up (u) and down (d) quarks is considered in the diquark spectator model. While the results of different articles in the literature suggest that the signs of the Boer-Mulders function in semi-inclusive deep inelastic scattering (SIDIS) for both flavors u and d are the same and negative, a previous calculation in the diquark spectator model found that $h_1^{\perp(u)}$ and $h_1^{\perp(d)}$ have different signs. The flavor dependence is of significance for the analysis of the azimuthal $\cos(2\phi)$ asymmetries in unpolarized SIDIS and Drell-Yan processes, as well as for the overall physical understanding of the distribution of transversely polarized quarks in unpolarized nucleons. We find substantial differences with previous work. In particular, we obtain half and first moments of the Boer-Mulders function that are negative over the full range in Bjorken x for both the u and d quarks. In conjunction with the Collins function, we then predict the $\cos(2\phi)$ azimuthal asymmetry for π^+ and π^- in this framework. We also find that the Sivers u and d quarks are negative and positive, respectively. As a by-product of the formalism, we calculate the chiral-odd but ''T-even'' function $h_{1L}^\perp$, which allows us to present a prediction for the single-spin asymmetry $A_{UL}^{\sin(2\phi)}$ for a longitudinally polarized target in SIDIS.

DOI: 10.1103/PhysRevD.77.094016 PACS numbers: 12.38.−t, 13.60.−r, 13.88.+e

I. INTRODUCTION

Naive time-reversal-odd (''T-odd'') transverse-momentum-dependent (TMD) parton distributions (PDFs) have gained considerable attention in recent years. Theoretically it is expected that they can account for nontrivial transverse spin and momentum correlations such as single-spin asymmetries (SSA) in hard scattering processes when transverse momentum scales are on the order of intrinsic transverse momentum of quarks in hadron, namely, $P_T \sim k_\perp \ll \sqrt{Q^2}$. Experiments are being performed [1–3] and proposed [4,5] to test these hypotheses by measuring transverse SSAs (TSSAs) and azimuthal asymmetries (AAs) in hard scattering processes such as semi-inclusive DIS (SIDIS) or the Drell-Yan process (DY). A prominent example of such a T-odd PDF is the Sivers function $f_{1T}^\perp$ [6,7] which explains the observed SSA in SIDIS for a transversely polarized proton target by the HERMES Collaboration [1]. It correlates the intrinsic quark transverse momentum and the transverse nucleon spin. The corresponding SSA on a deuteron target measured by COMPASS [2] vanishes, indicating a flavor dependence of the Sivers function.

Another leading twist T-odd parton distribution, introduced in [8], correlates the transverse spin of a quark with its transverse momentum within the nucleon, the so-called Boer-Mulders function $h_1^\perp$. It describes the distribution of transversely polarized quarks in an unpolarized nucleon.

Theoretically, twist-2 T-odd PDFs are of particular interest, as they formally emerge from the gauge link structure of the color gauge invariant definition of the quark-gluon-quark correlation function [9–11]. This gauge link not only ensures a color gauge invariant definition of correlation functions, but it also describes final state interactions (FSIs) [12] and initial state interactions [13] which are necessary to generate SSA [11,12,14]. Assuming factorization of leading twist SIDIS spin observables in terms of the ''T-even''[15] and T-odd TMD PDFs and fragmentation functions (FFs), Ref. [8] shows how spin observables in SIDIS can be expressed in terms of convolutions of these functions. Formal proofs of factorization of leading twist SIDIS spin observables were presented later in Refs. [16–18].

Apart from the leading twist transverse SSA, measurements were also performed in SIDIS on subleading SSA (i.e. they are suppressed like $1/Q$, where Q is the virtuality of the exchanged photon). In particular, the asymmetry for a longitudinally polarized target was measured by HERMES [19–22], whereas a nonvanishing beam-spin asymmetry was reported by CLAS [23,24]. It was shown that final state interactions contribute also to these types of single-spin asymmetries [25–28]. Subsequently, this effect was described by the introduction of heretofore unknown subleading twist T-odd PDFs [29]; a complete list of these PDFs was presented in Ref. [30]. These subleading twist T-odd PDFs discovered in this work were then incorporated into the tree-level formalism [31] completing the original work of [15].

In this paper we focus on the flavor dependence of the leading twist-2 T-odd parton distributions in semi-

inclusive DIS, i.e. the Boer-Mulders function $h_1^\perp$, which is also chirally odd, and the Sivers function $f_{1T}^\perp$ (keeping in mind that T-odd parton distributions in the Drell-Yan process flip their sign [9]). The Boer-Mulders function is particularly important for the analysis of the azimuthal $\cos(2\phi)$ asymmetry in unpolarized SIDIS and Drell-Yan processes. While in a partonic picture of the unpolarized $\cos(2\phi)$ asymmetry in SIDIS, the Boer-Mulders function is convoluted with the T-odd (and chiral-odd) Collins fragmentation function $H_1^\perp$ [32], the corresponding $\cos(2\phi)$ asymmetry in DY includes a convolution of the type $h_1^\perp \otimes \bar{h}_1^\perp$ [33] (where $\bar{h}_1^\perp$ is the Boer-Mulders function for antiquarks). Although these azimuthal asymmetries were measured in SIDIS by the ZEUS Collaboration [34,35] and in DY [36–38], little is known about the Boer-Mulders function. Of particular interest is the sign for different flavors u and d since this significantly affects predictions for these asymmetries (see Ref. [39]). The flavor dependence of $h_1^\perp$ was studied in the MIT-bag model [40] as well as in a spectator diquark model [41], and a large N_c analysis of TMDs was performed in Ref. [42]. Model calculations of chirally odd generalized parton distributions (GPDs) [43] and a study of generalized form factors in lattice QCD [44] give indications about the flavor dependence of $h_1^\perp$ by means of nonrigorous and model-dependent relations between GPDs and transverse-momentum-dependent PDFs which were proposed and discussed in Refs. [45–47]. All of these theoretical and phenomenological treatments suggest an equal (and negative) sign for the Boer-Mulders function for both u and d quarks, with the exception of the calculation in the diquark spectator model which results in opposite signs for u and d. The purpose of this paper is to consider the flavor dependence of $h_1^\perp$ and extend our earlier work on this subject [48,49]. Additionally, we consider the flavor dependence of the T-even function $h_{1L}^\perp$, which is also of interest in exploring the transverse momentum and quark spin correlations in a longitudinally polarized target [50].

II. T-ODD PDFS IN THE SPECTATOR MODEL

Transverse momentum quark distribution and fragmentation functions contain essential nonperturbative information about the partonic structure of hadrons. Practically speaking, their moments are calculable from first principles in lattice QCD. A great deal of understanding has also been gained from model calculations using the spectator framework. In addition to exploring the kinematics and pole structure of the TMDs [18,51,52], phenomenological estimates for parton distributions [53] and fragmentation functions [54] for T-even PDFs and for T-odd PDFs [12–14,28,41,47–49,55] have been performed. We extend these studies to explore the flavor dependence of the T-odd PDFs adopting the factorized approach used in Refs. [49,53,54].

We start (cf. [53]) from the definition of the fully unintegrated, color gauge invariant, quark-quark correlator

$$\Phi_{ij}(p;P,S) = \sum_X \int \frac{d^4\xi}{(2\pi)^4} e^{ip\cdot\xi} \langle P,S|\bar{\psi}_j(0)\mathcal{W}[0|\infty,0,\vec{0}_T]|X\rangle \times \langle X|\mathcal{W}[\infty,\xi^+,\vec{\xi}_T|\xi]\psi_i(\xi)|P,S\rangle, \quad (1)$$

where the gauge link indicated by the (straight) Wilson line is given by

$$\mathcal{W}[a|b] = \mathcal{P}\exp\left\{-ig\int_a^b ds^\mu A_\mu(s)\right\}. \quad (2)$$

In an arbitrary gauge there is a Wilson line at light-cone infinity pointing in transverse directions [10,11]. Here, we work in Feynman gauge where the transverse Wilson line vanishes [10]. In the definition (1) we insert a complete set of intermediate states $\mathbb{1} = \sum_x |X\rangle\langle X|$. In the diquark model the sum over a complete set of intermediate on-shell states $|X\rangle$ is represented by a single one-particle diquark state $|dq; p_{dq}, \lambda\rangle$, where p_{dq} is the diquark momentum and λ its polarization. Since the diquark is "built" from two valence quarks, it can be a spin 0 particle (scalar diquark) or a spin 1 particle (axial-vector diquark). By applying a translation on the second matrix element in Eq. (1), we can integrate out ξ, perform the momentum integration over the diquark momentum p_{dq}, and obtain

$$\Phi_{ij}(p;P,S) = \sum_\lambda \frac{\delta((P-p)^2 - m_s^2)\Theta(P^0-p^0)}{(2\pi)^3} \times \langle P,S|\bar{\psi}_j(0)\mathcal{W}[0|\infty,0,\vec{0}_T]|dq;P-p,\lambda\rangle \times \langle dq;P-p,\lambda|\mathcal{W}[\infty,0,\vec{0}_T|0]\psi_i(0)|P,S\rangle. \quad (3)$$

The essence of the diquark spectator model is to calculate the matrix elements in Eq. (3) by the introduction of effective nucleon-diquark-quark vertices.

For T-even parton distributions such as the unpolarized PDF f_1, one obtains a nonvanishing result at leading order (in the nucleon-diquark-quark coupling) with a trivial contribution from the Wilson line, i.e. at tree level. In this case the matrix element $\langle dq|\psi|P\rangle$ is depicted in the left panel of Fig. 1. For a scalar and an axial-vector diquark, different vertices have to be chosen. The most general nucleon-diquark-quark vertices for off-shell particles were presented in Ref. [56]. For the matrix elements $\langle dq|\psi|P\rangle$, the nucleon is on shell, which reduces the amount of structures of the vertices of Ref. [56]. In the following we work with the nucleon-diquark-quark vertices which were used in Ref. [53] to compute T-even PDFs. They read, for a scalar and an axial-vector diquark,

$$\Upsilon_s(N) = g_{sc}(p^2);\ \Upsilon_{ax}^\mu(N) = \frac{g_{ax}(p^2)}{\sqrt{3}}\gamma_5\left[\gamma^\mu - R_g\frac{P^\mu}{M}\right]. \quad (4)$$

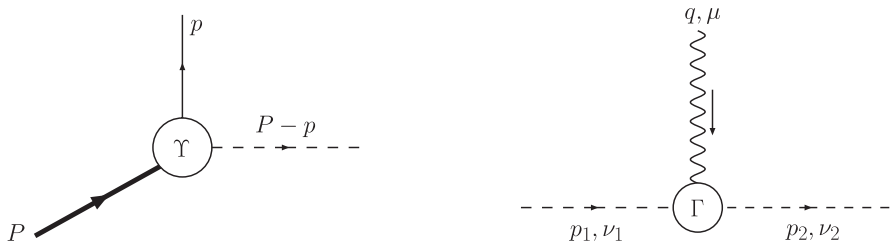

FIG. 1. Different vertices for the axial-vector diquark. Left panel: Nucleon-diquark-quark vertex. Right panel: Diquark-gluon vertex.

$g(p^2)$ are form factors depending on the quark momentum p. They are introduced to yield a more realistic description of the nonperturbative nature of the quark-quark correlator, and are specified below. R_g is a ratio of coupling constants, since both structures in the nucleon-(axial-vector)-diquark-quark coupling can, in principle, have different couplings.

To leading order, the matrix elements are given by the following expressions for a scalar and axial-vector diquark,

$$\langle sdq; P-p|\psi_i(0)|P,S\rangle = ig_{sc}(p^2)\frac{[(\not{p}+m_q)u(P,S)]_i}{p^2-m_q^2+i0}, \tag{5}$$

$$\begin{aligned}\langle adq; P-p;\lambda|\psi_i(0)|P,S\rangle &= i\frac{g_{ax}(p^2)}{\sqrt{3}}\varepsilon^*_\mu(P-p;\lambda)\\ &\times\frac{[(\not{p}+m_q)\gamma_5[\gamma^\mu - R_g\frac{P^\mu}{M}]u(P,S)]_i}{p^2-m_q^2+i0},\end{aligned} \tag{6}$$

where the polarization vector of the axial-vector diquark is given by ε_μ, $u(P,S)$ denotes the nucleon spinor, and M and m_q are nucleon and quark masses, respectively. In this paper we consider the diquark as a particle with mass m_s, and the polarization sum for the axial-vector diquark is

$$\begin{aligned}\sum_\lambda \varepsilon^*_\mu(P-p;\lambda)\varepsilon_\nu(P-p;\lambda)\\ = -g_{\mu\nu}+\frac{(P-p)_\mu(P-p)_\nu}{m_s^2}.\end{aligned} \tag{7}$$

The unpolarized TMD f_1 is obtained by inserting Eqs. (5) and (6) into Eq. (3) and projecting f_1 from the quark-quark correlator (see e.g. [30,31])

$$\begin{aligned}2f_1(x,\vec{p}_T^{\,2}) = \frac{1}{2}\int dp^-(\mathrm{Tr}[\gamma^+\Phi(p;P,S)]\\ +\mathrm{Tr}[\gamma^+\Phi(p;P,-S)])|_{p^+=xP^+},\end{aligned} \tag{8}$$

where the "+" sign of the γ matrix denotes the usual light-cone component [$a^\pm = 1/\sqrt{2}(a^0 \pm a^3)$]. The results for f_1 in the scalar and axial-vector diquark sectors read

$$\begin{aligned}f_1^{sc}(x,\vec{p}_T^{\,2}) = \frac{1}{2(2\pi)^3}|g_{sc}(p^2)|^2\frac{(1-x)}{[\vec{p}_T^{\,2}+\tilde{m}^2]^2}\\ \times[\vec{p}_T^{\,2}+(xM+m_q)^2],\end{aligned} \tag{9}$$

$$\begin{aligned}f_1^{ax}(x,\vec{p}_T^{\,2}) = \frac{1}{6(2\pi)^3}\frac{|g_{ax}(p^2)|^2}{M^2m_s^2(1-x)[\vec{p}_T^{\,2}+\tilde{m}^2]^2}\\ \times\mathcal{R}_1^{ax}(x,\vec{p}_T^{\,2};R_g,\{\mathcal{M}\}),\end{aligned} \tag{10}$$

where $\tilde{m}^2 \equiv xm_s^2 - x(1-x)M^2 + (1-x)m_q^2$. To shorten the notation we introduce a function $\mathcal{R}_1^{ax}$ depending on x and $\vec{p}_T$, and the model parameters R_g and the set of masses, i.e. $\{\mathcal{M}\} \equiv \{M, m_s, m_q\}$, to be fixed below.

Another T-even function of interest is the distribution of transversely polarized quarks in a longitudinally polarized target,

$$\begin{aligned}2\lambda_P p_T^i h_{1L}^\perp(x,\vec{p}_T^{\,2}) = \frac{M}{2}\int dp^-\{\mathrm{Tr}[\gamma^+\gamma^i\gamma_5\Phi(p;P,S_L)]\\ -\mathrm{Tr}[\gamma^+\gamma^i\gamma_5\Phi(p;P,-S_L)]\},\end{aligned} \tag{11}$$

where λ_P is the target helicity, and S_L is the spin 4-vector in the longitudinal direction, i.e. $S_L = [-\frac{\lambda_P}{M}P^-, \frac{\lambda_P}{M}P^+, \vec{0}_T]$. By applying the same methods as for f_1, we obtain

$$h_{1L}^{\perp,sc}(x,\vec{p}_T^{\,2}) = -\frac{|g_{sc}(p^2)|^2}{(2\pi)^3}\frac{(1-x)M(xM+m_q)}{[\vec{p}_T^{\,2}+\tilde{m}^2]^2}, \tag{12}$$

$$\begin{aligned}h_{1L}^{\perp,ax}(x,\vec{p}_T^{\,2}) = \frac{|g_{ax}(p^2)|^2}{12(2\pi)^3}\frac{1}{[\vec{p}_T^{\,2}+\tilde{m}^2]^2Mm_s^2(1-x)}\\ \times\mathcal{R}_{1L}^{\perp,ax}(x,\vec{p}_T^{\,2};R_g,\{\mathcal{M}\}),\end{aligned} \tag{13}$$

where for brevity $\mathcal{R}_1^{ax}$ and $\mathcal{R}_{1L}^{\perp,ax}$ are given in Appendix C.

By contrast, T-odd PDFs cannot be generated by simply considering the tree-level diagram in the left panel of Fig. 1. In the spectator framework the T-odd PDFs [12] are generated by the gauge link in Eq. (1) [13,14,48,49]. Thus, the leading contribution can be obtained by expanding the exponential of the gauge link up to first order. This contribution results in a box diagram as shown in the left panel of Fig. 2, which contains an imaginary part necessary for T-odd PDFs. We restrict ourselves to the case where one gluon models the final state interactions. The contribution of the gauge link is represented in the left panel of Fig. 2 by the double (eikonal) line and the eikonal vertex yielding a contribution to the box diagram

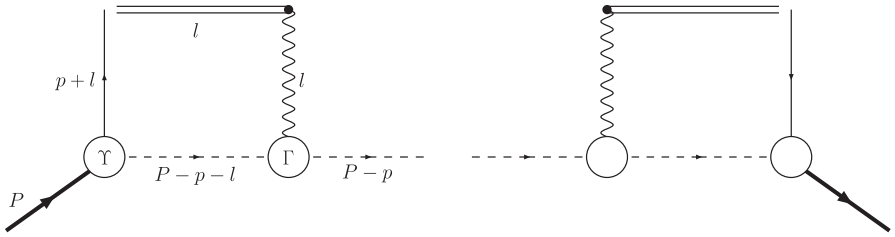

FIG. 2. Contribution of the gauge link in the one-gluon approximation. Left panel: Box graph. Right panel: Box graph Hermitian conjugated.

$$\frac{i}{[l\cdot v+i0]}\times(-ie_q v^\lambda), \tag{14}$$

where l is the loop momentum, e_q is the charge of the quark, and v is a light-cone vector representing the direction of the Wilson line. In order to evaluate the box diagram, we need to specify the gluon-diquark coupling. With a one-gluon exchange approximation in mind, we use the gluon-diquark coupling for a scalar diquark, and for an axial-vector diquark we use a general axial-vector-vector that models the composite nature of the diquark through an anomalous magnetic moment κ [57]. In the notations of Fig. 1 (right panel) the gluon-diquark vertices read

$$\Gamma_s^\mu = -ie_{dq}(p_1+p_2)^\mu, \tag{15}$$

$$\Gamma_{ax}^{\mu\nu_1\nu_2} = -ie_{dq}[g^{\nu_1\nu_2}(p_1+p_2)^\mu + (1+\kappa)\times(g^{\mu\nu_2}(p_2+q)^{\nu_1} + g^{\mu\nu_1}(p_1-q)^{\nu_2})]. \tag{16}$$

For $\kappa=-2$ the vertex Γ_{ax} reduces to the standard γWW vertex. We can now express the matrix elements including the gauge link in the one-gluon approximation in the following way:

$$\langle sdq;P-p|\mathcal{W}[\infty,0,\vec{0}_T|0]\psi_i(0)|P,S\rangle|_{1-gl} = -ie_q e_{dq}\int\frac{d^4l}{(2\pi)^4}g_{sc}((l+p)^2)\mathcal{D}^{sc}(P-p-l)\times\frac{[(\not p+\not l+m_q)u(P,S)]_i v\cdot(2P-2p-l)}{[l\cdot v+i0][l^2+i0][(l+p)^2-m_q^2+i0]}, \tag{17}$$

$$\langle adq;P-p,\lambda|\mathcal{W}[\infty,0,\vec{0}_T|0]\psi_i(0)|P,S\rangle|_{1-gl} = -ie_q e_{dq}\int\frac{d^4l}{(2\pi)^4}\frac{g_{ax}((p+l)^2)}{\sqrt{3}}\varepsilon_\sigma^*(P-p,\lambda)\mathcal{D}_{\rho\eta}^{ax}(P-p-l)\times\frac{[g^{\sigma\rho}v\cdot(2P-2p-l)+(1+\kappa)(v^\sigma(P-p+l)^\rho+v^\rho(P-p-2l)^\sigma)]}{[l\cdot v+i0][l^2+i0][(l+p)^2-m_q^2+i0]}\times\left[(\not p+\not l+m_q)\gamma_5\left(\gamma^\eta-R_g\frac{P^\eta}{M}\right)u(P,S)\right]_i, \tag{18}$$

where the subscript $1-gl$ denotes "one gluon exchange." In these expressions $\mathcal{D}$ denotes the propagator of the scalar and axial-vector diquark,

$$\mathcal{D}^{sc}(P-p-l) = \frac{i}{[(P-p-l)^2-m_s^2+i0]}, \tag{19}$$

$$\mathcal{D}_{\mu\nu}^{ax}(P-p-l) = \frac{-i(g_{\mu\nu}-\frac{(P-p-l)_\mu(P-p-l)_\nu}{m_s^2})}{[(P-p-l)^2-m_s^2+i0]}. \tag{20}$$

The term $\frac{(P-p-l)_\mu(P-p-l)_\nu}{m_s^2}$ is a crucial difference of our approach compared to the calculation in Ref. [41], where the dependence on the proton and spectator momenta inside the loop integral is absent. It is shown below that this leads to various complications when performing the loop integral.

In a similar fashion as for f_1 and $h_{1L}^\perp$, we extract the Boer-Mulders function by inserting Eqs. (17) and (18) [and the tree-matrix elements (5) and (6), i.e. the leading nontrivial perturbative contribution is the interference term between tree graph and box graph] into the quark-quark correlator (3),

$$2\epsilon_T^{ij}p_T^j h_1^\perp(x,\vec{p}_T^{\,2}) = \frac{M}{2}\int dp^-(\mathrm{Tr}[\Phi_{\mathrm{unpol}}(p,S)i\sigma^{i+}\gamma_5] + \mathrm{Tr}[\Phi_{\mathrm{unpol}}(p,-S)i\sigma^{i+}\gamma_5])|_{p^+=xP^+}, \tag{21}$$

where $\epsilon_T^{ij}\equiv\epsilon^{-+ij}$ and $\epsilon^{0123}=+1$.

III. BOER-MULDERS FUNCTION FOR AN AXIAL-VECTOR DIQUARK

We proceed with calculating the Boer-Mulders function in the axial-vector diquark sector. As described above, the interference term between the tree and box graphs reads

$$\epsilon_T^{ij} p_T^j h_1^{\perp,ax}(x,\vec{p}_T^{\,2}) = -\frac{e_q e_{dq}}{8(2\pi)^3}\frac{1}{\vec{p}_T^{\,2}+\tilde{m}^2}\frac{M}{P^+}\int\frac{d^4l}{(2\pi)^4}\Big\{\frac{1}{3}g_{ax}((l+p)^2)g_{ax}^*(p^2)\mathcal{D}_{\rho\eta}(P-p-l)\Big(\sum_\lambda \varepsilon_\sigma^*(P-p;\lambda)\varepsilon_\mu \times(P-p;\lambda)\Big)\frac{[g^{\sigma\rho}v\cdot(2P-2p-l)+(1+\kappa)(v^\sigma(P-p+l)^\rho+v^\rho(P-p-2l)^\sigma)]}{[l\cdot v+i0][l^2-\lambda^2+i0][(l+p)^2-m_q^2+i0]} \times \mathrm{Tr}\Big[(\not{P}+M)\Big(\gamma^\mu - R_g\frac{P^\mu}{M}\Big)(\not{p}-m_q)\gamma^+\gamma^i(\not{l}+\not{p}+m_q)\Big(\gamma^\eta+R_g\frac{P^\eta}{M}\Big)\gamma_5\Big]\Big\} + \text{H.c.} \tag{22}$$

The momentum of the quark, p, is specified by

$$p = \Big[p^- = -\frac{\vec{p}_T^{\,2}+m_s^2-(1-x)M^2}{2(1-x)P^+},\ p^+ = xP^+,\ \vec{p}_T\Big]. \tag{23}$$

A. Light-cone integration

Here we comment on the evaluation of the four-dimensional loop integral in Eq. (22). A convenient way to simplify the calculation is to sort the numerator in terms of loop momenta and consider each term separately. Since the numerator in Eq. (22) contains at most the loop momentum to the power of 4, we can write it in the following way:

$$\text{numerator} = \sum_{i=1}^{4} N^{(i)}_{\alpha_1\ldots\alpha_i} l^{\alpha_1}\ldots l^{\alpha_i} + N^{(0)}. \tag{24}$$

The (real) coefficients (tensors) $N^{(i)}_{\alpha_1\ldots\alpha_i}$ depend only on external momenta P (nucleon momentum) and p (quark momentum) and can be computed in a straightforward but tedious calculation. We used the MATHEMATICA package TRACER [58] for this decomposition (24). The advantage of this procedure is that we are left with an arbitrary integral of the form

$$J^{(i)\alpha_1\alpha_2\ldots\alpha_i} \equiv \int\frac{d^4l}{(2\pi)^4}\frac{\frac{1}{3}g_{ax}((l+p)^2)g_{ax}^*(p^2)l^{\alpha_1}l^{\alpha_2}\ldots l^{\alpha_i}}{[l\cdot v+i0][l^2-\lambda^2+i0][(l+p-P)^2-m_s^2+i0][(l+p)^2-m_q^2+i0]}, \tag{25}$$

and the light-cone components of the loop momentum, l^+ and l^-, can be integrated out easily.

We sketch the light-cone integration. First, we specify the vector v to be a light-cone vector $v = [v^- = 1, v^+ = 0, \vec{v}_T = 0]$ representing the Wilson line. Thus, the product $l\cdot v$ reduces to l^+ and does not contribute to the l^- integration. Next, we perform the integral over l^- via contour integration and encounter three poles in the l^- plane from the last three terms in the denominator in Eq. (25). The integral is nonvanishing when $-xP^+ < l^+ < (1-x)P^+$; otherwise all poles are located in the same complex l^- half-plane. For $-xP^+ < l^+ < (1-x)P^+$ the third factor in the denominator in Eq. (25) always has a positive imaginary part, while the fourth factor always has a negative one. The imaginary part of the second factor becomes positive for $l^+ < 0$ and negative for $l^+ > 0$. We close the contour of integration in the upper half-plane which excludes the fourth factor in the denominator, and the second for $l^+ > 0$. Thus, we obtain

$$\begin{aligned} J^{(i)\alpha_1\ldots\alpha_i} = {} & \frac{1}{3}i\int\frac{d^2\vec{l}_T}{(2\pi)^2}\int_{-xP^+}^{(1-x)P^+}\frac{dl^+}{2\pi}\frac{1}{[l^+ + i0]} \\ & \times\frac{1}{[2l^+(2(l^+-(1-x)P^+)(P^- - p^-)+[(\vec{l}_T+\vec{p}_T)^2+m_s^2])-2(l^+-(1-x)P^+)[\vec{l}_T^{\,2}+\lambda^2]]} \\ & \times\Big\{\frac{[2(l^+-(1-x)P^+)][g_{ax}((l+p)^2)g_{ax}^*(p^2)(l^{\alpha_1}\ldots l^{\alpha_i})]|_{l^-=P^- - p^- +((\vec{l}_T+\vec{p}_T)^2+m_s^2)/2(l^+-(1-x)P^+)}}{[2(l^+-(1-x)P^+)(2(l^++xP^+)P^- -[(\vec{l}_T+\vec{p}_T)^2+m_q^2])+2(l^++xP^+)[(\vec{l}_T+\vec{p}_T)^2+m_s^2]]} \\ & -\frac{[2l^+]\Theta(-l^+)[g_{ax}((l+p)^2)g_{ax}^*(p^2)(l^{\alpha_1}\ldots l^{\alpha_i})]|_{l^-=(\vec{l}_T^{\,2}+\lambda^2)/2l^+}}{[2l^+(2(l^++xP^+)p^- -[(\vec{l}_T+\vec{p}_T)^2+m_q^2])+2(l^++xP^+)[\vec{l}_T^{\,2}+\lambda^2]]}\Big\}. \end{aligned} \tag{26}$$

We calculate the l^+ integral by adding the complex conjugated integral (stemming from the complex conjugated interference graph). Since $1/(l^+ + i0)$ is the only propagator remaining with an imaginary part, adding the complex conjugated integral results in a δ-function contribution via the relation

$$\frac{1}{l^+ + i0} - \frac{1}{l^+ - i0} = -2\pi i \delta(l^+). \tag{27}$$

We obtain

$$J^{(i)\alpha_1\ldots\alpha_i} + (J^{(i)\alpha_1\ldots\alpha_i})^* = \frac{1}{3}\int \frac{d^2\vec{l}_T}{(2\pi)^2}\left\{\frac{(-1)(g_{ax}((l+p)^2)g^*_{ax}(p^2)[l^{\alpha_1}\ldots l^{\alpha_i}])|_{l^-=((\vec{p}_T^{\,2}-(\vec{l}_T+\vec{p}_T)^2)/2(1-x)P^+),l^+=0}}{2P^+[\vec{l}_T^{\,2}+\lambda^2][(\vec{l}_T+\vec{p}_T)^2+\tilde{m}^2]}\right.$$
$$\left. - \int_{-xP^+}^{(1-x)P^+} dl^+\left[\frac{[\frac{l^+}{xP^+}]\Theta(-l^+)\delta(l^+)(g_{ax}((l+p)^2)g^*_{ax}(p^2)[l^{\alpha_1}\ldots l^{\alpha_i}])|_{l^-=(\vec{l}_T^{\,2}+\lambda^2)/2l^+}}{[2(1-x)P^+[\vec{l}_T^{\,2}+\lambda^2]][\vec{l}_T^{\,2}+\lambda^2]}\right]\right\}. \tag{28}$$

At this point we are forced to specify the form factor g_{ax} since the second integral in Eq. (28) is potentially ill defined. This happens when $g(p^2)$ is a holomorphic function in p^2 (i.e. it contains no poles) and at least one of the Minkowski indices is lightlike in the minus direction, e.g. $\alpha_1 = -$, $\alpha_2, \ldots, \alpha_i \in \{+, \perp\}$. In such cases we end up with an integral of the form $\int dl^+ \delta(l^+)\Theta(-l^+)$, which is ill defined. This implies that $l^+ = 0$ and $l^- = \infty$, which signals the existence of a light-cone divergence as was shown in Ref. [55]. While for a *scalar* diquark one does not encounter a Minkowski index, $\alpha_j = -$, for twist-2 T-odd PDFs such as the Boer-Mulders function (so that there are no light-cone divergences in this case), it was shown in Ref. [55] that for twist-3 T-odd PDFs light-cone divergences exist for a scalar diquark. However, calculating the coefficients $N^{(i)}_{\alpha_1\ldots\alpha_i}$ in Eq. (24) for an axial-vector diquark, one of the Minkowski indices can be a "minus" (i.e. $\alpha_j = -$). Thus, for an axial-vector diquark we encounter a light-cone divergence already for twist-2 T-odd PDFs. Here it is worth mentioning that such divergences do not arise in a pQCD-quark-target model where the spectator state is a gluon [59].

From the standpoint of phenomenology one can regard these light-cone divergences as model artifacts (for the axial-vector diquark model). It was shown in Ref. [55] how to regularize these light-cone divergences by introducing a non-lightlike Wilson line. It was pointed out that one can also handle the light-cone divergences by introducing phenomenological form factors with additional poles. Like the quark propagator in Eq. (22) they introduce additional factors of l^+ in the numerator of the second term in Eq. (28). We adopt this procedure to model the Boer-Mulders function and choose a form factor of the following form:

$$g_{ax}(p^2) = N_{ax}^{n-1}\frac{(p^2 - m_q^2)f(p^2)}{[p^2 - \Lambda^2 + i0]^n}, \tag{29}$$

and find that for $n \geq 3$ (for $n \geq 2$ it is already sufficient for $\kappa = -2$) enough powers of l^+ enter the numerator of the second term in Eq. (28) to compensate the minus components l^-. The second term then vanishes since $\int dl^+ l^{+n}\delta(l^+)\Theta(-l^+) = 0$ for $n \geq 1$. In Eq. (29) $f(p^2)$ is then a function without poles to be fixed below, while Λ is an arbitrary mass scale to be fixed by phenomenology (i.e. fitting f_1 to data). N_{ax} is a normalization factor.

After performing the light-cone integrations we are then left with the remaining integral over the transverse loop momentum (for $n = 3$),

$$\epsilon_T^{ij}p_T^j h_1^{\perp,ax}(x,\vec{p}_T^{\,2}) = -\frac{e_q e_{dq}}{8(2\pi)^3}N_{ax}^4\frac{1}{3}\frac{(1-x)^3 f(p^2)}{[\vec{p}_T^{\,2}+\tilde{m}_\Lambda^2]^3 m_s^4}\int\frac{d^2\vec{l}_T}{(2\pi)^2}\frac{f^*((p+l)^2)}{[\vec{l}_T^{\,2}+\lambda^2][(\vec{l}_T+\vec{p}_T)^2+\tilde{m}_\Lambda^2]^3}\{\epsilon_T^{ij}p_T^j[(\vec{l}_T^{\,2})^2 A_p$$
$$+ 2(\vec{l}_T\cdot\vec{p}_T)\vec{l}_T^{\,2}B_p + \vec{l}_T^{\,2}C_p + 2(\vec{l}_T\cdot\vec{p}_T)D_p + E_p] + \epsilon_T^{ij}l_T^j[(\vec{l}_T^{\,2})^2 A_l + 2(\vec{l}_T\cdot\vec{p}_T)\vec{l}_T^{\,2}B_l + \vec{l}_T^{\,2}C_l$$
$$+ 2(\vec{l}_T\cdot\vec{p}_T)D_l + E_l] + \epsilon_T^{rs}l_T^r p_T^s[(A_{lp}\vec{l}_T^{\,2} + 2\vec{l}_T\cdot\vec{p}_T B_{lp})(l_T^i + p_T^i) + E_{lp}(l_T^i + 2p_T^i)]\}, \tag{30}$$

where the coefficients which are functions of x, M, m_q, p_T^2, κ, and R_g are given in Appendix A. $\tilde{m}_\Lambda^2$ replaces $\tilde{m}^2$ by $\tilde{m}_\Lambda^2 = xm_s^2 - x(1-x)M^2 + (1-x)\Lambda^2$. We point out that the vanishing of the coefficient E_p *ensures that no IR divergence appears in the transverse integral* (30). This serves as an important check of the calculation.

B. Transverse integral

The transverse integral (30) can be calculated in a straightforward manner. We note that the transverse integral (30) is UV divergent if we choose $f(p^2) = 1$. This can be seen from naive power counting of the integrand. The UV divergence stems from the term $\vec{l}_T^{\,4}$, which in turn is a

consequence of the fact that we took the full numerator of the axial-vector diquark propagator into account, in contrast to Ref. [41] where no UV divergences were reported. We regularize it by choosing $f(p^2)$ to be a covariant Gaussian,

$$f((l+p)^2) = \mathrm{e}^{-b|l+p|^2}, \tag{31}$$

where b is interpreted as the regulator of the high l integration. Because of the pole contribution $l^+ = 0$, the Gaussian has no effect on the light-cone integration. Thus we can write the squared products of the momenta $l+p$ and p—after performing the light-cone integration—as follows,

$$(l+p)^2 = -\frac{(\vec{l}_T + \vec{p}_T)^2 + x m_s^2 - x(1-x)M^2}{1-x}, \tag{32}$$

$$p^2 = -\frac{\vec{p}_T^{\,2} + x m_s^2 - x(1-x)M^2}{1-x}. \tag{33}$$

Now all that remains is to perform the $\vec{l}_T$ integration. After a shift of the integration variable from $\vec{l}_T \to \vec{l}_T + \vec{p}_T$, it is convenient to use polar coordinates to calculate the integral, and perform the angular integration first. For this we choose a coordinate system in such a way that the x axis is along $\vec{p}_T$, such that $\vec{p}_T = |\vec{p}_T|(1,0)$. The integration is performed with respect to that direction, i.e. $\vec{l}_T = |\vec{l}_T|(\cos\phi, \sin\phi)$. Having fixed the coordinate system in such a way, the hanging index i can only be 2. We perform now the angular integration over ϕ by means of the formula

$$\int_0^\pi \frac{\cos(nx)dx}{1+a\cos(x)} = \frac{\pi}{\sqrt{1-a^2}}\left(\frac{\sqrt{1-a^2}-1}{a}\right)^n, \qquad a^2 < 1, \quad n \geq 0. \tag{34}$$

We are left with the remaining one-dimensional integrals ($\sqrt{z} \equiv l$)

$$\begin{aligned} h_1^{\perp,ax}(x,\vec{p}_T^{\,2}) = &-\frac{e_q e_{dq}}{48(2\pi)^4} N_{ax}^4 \frac{(1-x)^3 \mathrm{e}^{-\tilde{b}(\vec{p}_T^{\,2} + 2x m_s^2 - 2x(1-x)M^2)}}{m_s^4[\vec{p}_T^{\,2} + \tilde{m}_\Lambda^2]^3} \left(\int_0^\infty \frac{\mathrm{e}^{-\tilde{b}z}dz}{[z+\tilde{m}_\Lambda^2]^3}[z(A_p - 2A_l + B_l) + \vec{p}_T^{\,2}(A_p - A_l \right. \\ &- 2(B_p - B_l)) + C_p - C_l] + \int_0^{\vec{p}_T^{\,2}} \frac{\mathrm{e}^{-\tilde{b}z}dz}{[z+\tilde{m}_\Lambda^2]^3}\left[z^2 \frac{A_{lp}}{2\vec{p}_T^{\,2}} + z\left(-\frac{1}{2}A_{lp} - \frac{D_l}{\vec{p}_T^{\,2}} + \frac{E_{lp}}{2\vec{p}_T^{\,2}}\right) - 2(D_p - D_l) - \frac{E_l}{\vec{p}_T^{\,2}}\right] \\ &\left. + \int_{\vec{p}_T^{\,2}}^\infty \frac{\mathrm{e}^{-\tilde{b}z}dz}{[z+\tilde{m}_\Lambda^2]^3}\left[z\frac{A_{lp}}{2} - \vec{p}_T^{\,2}\frac{A_{lp}}{2} + D_l + \frac{1}{2}E_{lp}\right]\right), \end{aligned} \tag{35}$$

where $\tilde{b} \equiv b/(1-x)$. These integrals can be expressed in terms of incomplete Γ functions,

$$\Gamma(n,x) \equiv \int_x^\infty \mathrm{e}^{-t} t^{n-1} dt. \tag{36}$$

The Boer-Mulders function for an axial-vector diquark then reads

$$\begin{aligned} h_1^{\perp,ax}(x,\vec{p}_T^{\,2}) = &-\frac{e_q e_{dq}}{48(2\pi)^4} N_{ax}^4 \frac{(1-x)^3 \mathrm{e}^{-\tilde{b}\vec{p}_T^{\,2} - 2\tilde{b}(x m_s^2 - x(1-x)M^2)}}{m_s^4[\vec{p}_T^{\,2} + \tilde{m}_\Lambda^2]^3} \\ &\times \mathcal{R}_1^{\perp,ax}(x,\vec{p}_T^{\,2}; R_g, \kappa, \tilde{b}, \Lambda, \{\mathcal{M}\}), \end{aligned} \tag{37}$$

where the explicit form of $\mathcal{R}_1^\perp$ is expressed in terms of incomplete Gamma functions and can be found in Appendix C.

The Boer-Mulders function for a scalar diquark is much easier to calculate [48] due to its simpler Dirac-trace structure. The light-cone divergences we have encountered in the axial-vector diquark sector do not appear for the scalar sector. With our choice of the form factor [cf. Eqs (29) and (31)] the Boer-Mulders function for a scalar diquark reads

$$\begin{aligned} h_1^{\perp,sc}(x,\vec{p}_T^{\,2}) = &\frac{e_q e_{dq}}{4(2\pi)^4} N_{sc}^4 \frac{(1-x)^5 M(xM+m_q)}{\vec{p}_T^{\,2}[\vec{p}_T^{\,2} + \tilde{m}_\Lambda^2]^3} \\ &\times \mathrm{e}^{-\tilde{b}(\vec{p}_T^{\,2} + 2x m_s^2 - 2x(1-x)M^2)}\left[\frac{\tilde{b}^2}{2}\mathrm{e}^{\tilde{b}\tilde{m}_\Lambda^2}(\Gamma(0,\tilde{b}\tilde{m}_\Lambda^2) \right. \\ &- \Gamma(0,\tilde{b}(\vec{p}_T^{\,2} + \tilde{m}_\Lambda^2)) + \frac{1-\tilde{b}\tilde{m}_\Lambda^2}{2\tilde{m}_\Lambda^4} \\ &\left. - \frac{1-\tilde{b}(\vec{p}_T^{\,2} + \tilde{m}_\Lambda^2)}{2(\vec{p}_T^{\,2} + \tilde{m}_\Lambda^2)^2}\mathrm{e}^{-\tilde{b}\vec{p}_T^{\,2}}\right]. \end{aligned} \tag{38}$$

C. Sivers function in the diquark spectator model

Having obtained the results for the Boer-Mulders function $h_1^\perp$, it is straightforward to apply the procedure described above to calculate the Sivers function $f_{1T}^\perp$. The Sivers function can be extracted from the following trace of the quark-quark correlator (3) (see e.g. [30,31]),

$$\begin{aligned} 2S_T^i \epsilon_T^{ij} p_T^j f_{1T}^\perp(x,\vec{p}_T^{\,2}) = &\frac{M}{2}\int dp^- (\mathrm{Tr}[\gamma^+ \Phi(p;P,S_T)] \\ &- \mathrm{Tr}[\gamma^+ \Phi(p;P,-S_T)])|_{p^+ = xP^+}. \end{aligned} \tag{39}$$

It is well known [48] that in the scalar diquark spectator sector the Boer-Mulders function and the Sivers function coincide, so the scalar Sivers function is given by the left-hand side of Eq. (38). By contrast the different Dirac structure for the chiral even Sivers function and the chiral-odd Boer-Mulders function in the axial-vector diquark sector, Eqs. (21) and (22), respectively, leads to different coefficients in the decomposition $N^{(i)}_{\alpha_1\ldots\alpha_i}$ in Eq. (24). So, whereas the form of the Sivers function $f_{1T}^{\perp,ax}$ is the same as the form of $h_1^{\perp,ax}$ given in Eq. (37), the coefficients A_p, B_p, C_p, D_p, E_p, A_l, B_l, C_l, D_l, E_l, A_{lp}, B_{lp}, E_{lp} differ. They are given for $f_{1T}^{\perp,ax}$ explicitly in Appendix B.

IV. ASYMMETRIES IN SIDIS

A. Azimuthal $\cos(2\phi)$ asymmetry in unpolarized SIDIS

Almost 30 years ago it was pointed out that both kinematic [60] and dynamical effects [61,62] could give rise to a $\cos 2\phi$ azimuthal asymmetry going like p_T^2/Q^2 (where Q is a hard scale) when transverse momentum scales are on the order of the intrinsic momentum scales of partons, $P_T \sim p_T$. However, when transverse momentum is on the order of the hard scale, $P_T \sim Q$, these nonperturbative effects are expected to decrease relative to perturbative contributions [63,64]. By contrast, taking into account the existence of T-odd TMDs and fragmentation functions, it was pointed out by Boer and Mulders [8] that at leading twist a convolution of the Boer-Mulders and the Collins functions would give rise to nontrivial azimuthal asymmetries in unpolarized SIDIS.

Having explored the flavor dependence of the $h_1^\perp$, we are now in a position to extend early phenomenological work on T-odd contributions to azimuthal asymmetries in SIDIS performed under the approximation of scalar diquark dominance [49]. In particular, we consider the spin-independent double T-odd $\cos 2\phi$ asymmetry for π^+ and π^- production.

The general form of the cross section for an unpolarized target reads [31]

$$\frac{d\sigma}{dxdydzd\phi_h dP_{h\perp}^2} \approx \frac{2\pi\alpha^2}{xyQ^2}\Big[\Big(1-y+\frac{1}{2}y^2\Big)F_{UU,T} + (1-y)F_{UU,L} + (2-y)\cos(\phi_h)F_{UU}^{\cos\phi} + (1-y)\cos(2\phi_h)F_{UU}^{\cos 2\phi_h}\Big], \quad (40)$$

where the structure function $F_{UU}^{\cos 2\phi_h}$ is of the most interest for the purpose of this paper. At leading twist it factorizes into a convolution of the Boer-Mulders and Collins fragmentation function [16,31],

$$F_{UU}^{\cos 2\phi_h} = \mathcal{C}\Big[-\frac{2\hat{\boldsymbol{h}}\cdot\boldsymbol{k}_T\hat{\boldsymbol{h}}\cdot\boldsymbol{p}_T - \boldsymbol{k}_T\cdot\boldsymbol{p}_T}{MM_h}h_1^\perp H_1^\perp\Big]. \quad (41)$$

The convolution integral $\mathcal{C}$ is given by

$$\mathcal{C}[wfD] = x\sum_a e_a^2\int d^2\boldsymbol{p}_T d^2\boldsymbol{k}_T\delta^{(2)}(\boldsymbol{p}_T - \boldsymbol{k}_T - \boldsymbol{P}_{h\perp/z}) \times w(\boldsymbol{p}_T,\boldsymbol{k}_T)f^a(x,p_T^2)D^a(z,k_T^2), \quad (42)$$

where summation runs over quarks and antiquarks. $\boldsymbol{p}_T$, $\boldsymbol{k}_T$ are the intrinsic transverse momenta of the active and fragmenting quarks, respectively, and $\boldsymbol{P}_h$ is the transverse momentum of the fragmenting hadron with respect to the photon momentum q. $\hat{\boldsymbol{h}}$ is defined as $\boldsymbol{P}_{h\perp}/|\boldsymbol{P}_{h\perp}|$.

We have fixed most of the model parameters, such as masses and normalizations, by comparing the model result for the unpolarized T-even PDF f_1 for u and d quarks [Eqs. (9) and (10)] to the leading order (LO) low-scale ($\mu^2 = 0.26$ GeV) data parametrization of Glück, Reya, and Vogt (GRV) [65]. Note that PDFs for u and d quarks are given by linear combinations of PDFs for an axial vector and scalar diquark, $u = \frac{3}{2}f^{sc} + \frac{1}{2}f^{ax}$ and $d = f^{ax}$ [41,53]. The best model approximation to the GRV data parametrization for u and d of [65] is shown in Fig. 3, and corresponds to a set of parameters $m_q = 0$ GeV, $m_s = 1.0$ GeV, $m_{ax} = 1.3$ GeV, $\Lambda = 1.3$ GeV, $M = 0.94$ GeV – fixed, and $R_g = 5/4$. For T-odd PDFs such a procedure for fixing the model parameters is not sufficient since it does not determine the sign and the strength of the final state interactions. In our case the final state interactions are described effectively in the one-gluon exchange approximation by the product $e_{dq}e_q$, the charges of the diquark and quark, respectively. We need to fix the value of this product. For that reason we calculated the Sivers function for u and d quarks in the diquark model and compared our results in Fig. 3 for the "one-half" moment,

$$f_{1T}^{\perp(q,1/2)}(x) = \int d^2p_T\frac{|\vec{p}_T|}{M}f_{1T}^{\perp(q)}(x,\vec{p}_T^{\,2}), \quad (43)$$

as well as the first moment,

$$f_{1T}^{\perp(q,1)}(x) = \int d^2p_T\frac{\vec{p}_T^{\,2}}{2M^2}f_{1T}^{\perp(q)}(x,\vec{p}_T^{\,2}), \quad (44)$$

with the existing data parametrizations where q represents the quark flavor (see Refs. [66–70]). In such a way we are able to fix $e_{dq}e_q/4\pi = C_F\alpha_s = 0.267$[1] with a color factor, $C_F = 4/3$. We display the one-half and first moments for u- and d-quark Sivers functions $f_{1T}^{\perp(q)}$ and Boer-Mulders functions $h_1^{\perp(q)}$ (where $q = u, d$) along with the unpolarized u- and d-quark PDFs in Figs. 4 and 5. The one-half and first moments of the u- and d-quark Sivers functions are negative and positive, respectively, while the u- and

[1]This is in agreement with the value α_s used in [71] to explore the T-odd fragmentation functions. It is worth noting that the running coupling extrapolated to the "low-scale" μ^2 in [65] is different than the coupling that characterizes the FSIs in the one-gluon exchange approximation.

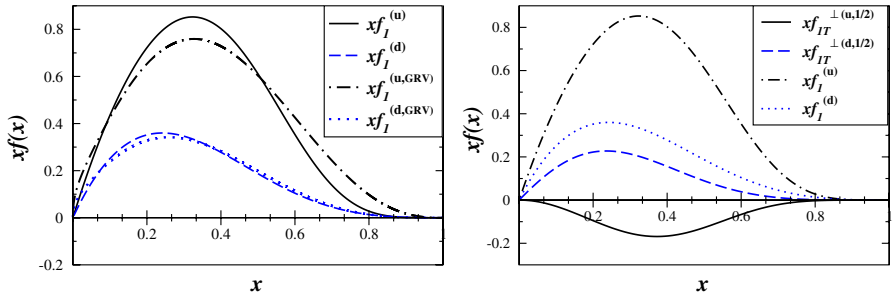

FIG. 3 (color online). Left panel: The unpolarized u- and d-quark distributions functions versus x compared to the low-scale parametrization of the unpolarized u- and d-quark distributions [65]. Right panel: The half-moment of the Sivers functions and the unpolarized u and d distributions versus x compared to the low-scale parametrization of the unpolarized u- and d-quark distributions ($\kappa = 1.0$).

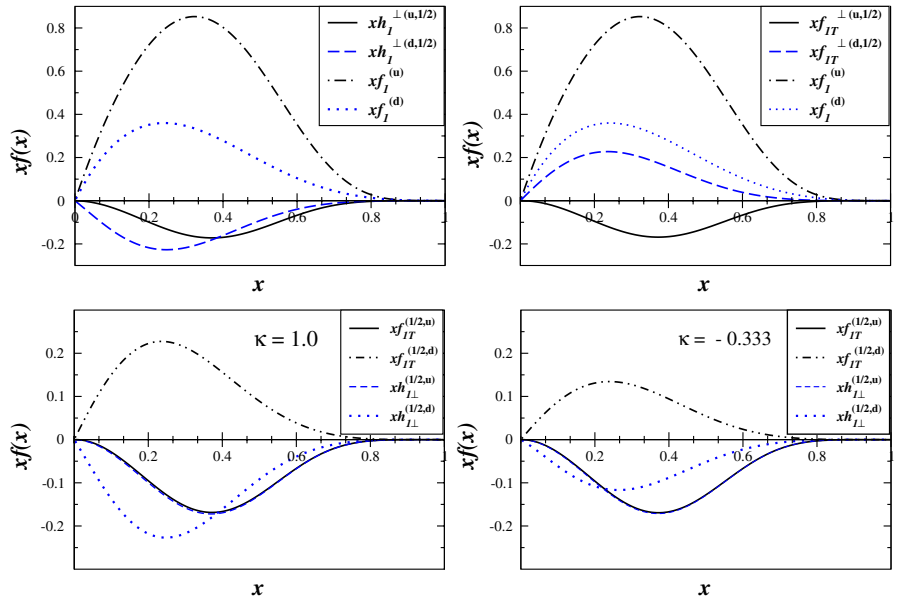

FIG. 4 (color online). Top panels: The half-moments of the Boer-Mulders (left) and Sivers (right) functions versus x compared to the unpolarized u- and d-quark distribution functions. Bottom panels: The half-moments of the Boer-Mulders and Sivers functions, $\kappa = 1.0$ (lower left), $\kappa = -0.333$ (lower right), versus x, extractions from data were presented in Refs. [66–70] for the Sivers function.

d-quark Boer-Mulders functions are both negative over the full range in Bjorken x. These results are in agreement with the large N_c predictions [42], the bag model results reported in [40], the impact parameter distortion picture of Burkardt [45], and recent studies of nucleon transverse spin structure in lattice QCD [44].[2] Also, we explored the relative dependence of the d-quark to u-quark Sivers functions; see Fig. 4. For example, choosing a value of $\kappa = -0.333$ as was determined in Ref. [57], we find the d-quark Sivers function is smaller than the u-quark one. Choosing $\kappa = 1$ we find reasonable agreement with extractions reported in [66]. It is worth noting (see Fig. 4) that the resulting u-quark Sivers function and Boer-Mulders function are nearly equal, even with the inclusion of the axial-vector spectator diquark. An exact equality was first noted in the simpler scalar diquark dominance approximation in [48].

Our model input for the Collins functions is based on very recent work in [71] where the Collins function was calculated in the spectator framework. Therein it was assumed that $H_1^{\perp(\mathrm{dis-fav})} \approx -H_1^{\perp(\mathrm{fav})}$ in the pion sector, thereby satisfying the Schäfer-Teryaev sum rule [72] locally. We use those results along with the results of this

[2]It is interesting to note that the approximate agreement for the flavor dependence of $h_1^\perp$ among such models probably arises because our input quark and diquark wave functions share the same SU(4) flavor-spin dependence as the bag and other spectator models. Additionally SU(4) symmetric baryon wave functions are compatible with large-N_c counting rules.

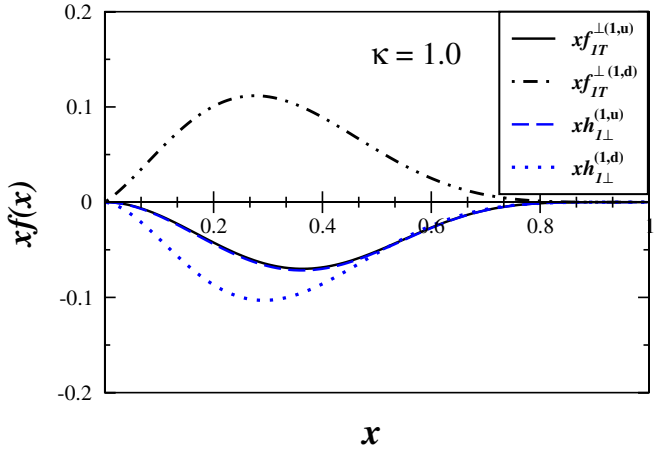

FIG. 5 (color online). The first moment of the Boer-Mulders and Sivers functions versus x for $\kappa = 1.0$.

paper for $h_1^\perp$ to estimate the azimuthal asymmetry $A_{UU}^{\cos 2\phi}$ [cf. Eq. (41)], where

$$A_{UU}^{\cos 2\phi} \equiv \frac{\int d\Phi \cos 2\phi d\sigma}{\int d\Phi d\sigma} \tag{45}$$

and $d\Phi$ is shorthand notation for the phase space integration. In Fig. 6 we display the $A_{UU}^{\cos 2\phi}(P_T)$ in the range of future JLab kinematics [73] ($0.08 < x < 0.7$, $0.2 < y < 0.9$, $0.3 < z < 0.8$, $Q^2 > 1$ GeV$/c$, and $1 < E_\pi < 9$ GeV) and HERMES kinematics [1] ($0.23 < x < 0.4$, $0.1 < y < 0.85$, $0.2 < z < 0.7$, with $Q^2 > 1$ GeV$/c$ and $4.5 < E_\pi < 13.5$ GeV). In Fig. 7 we display the x and z dependence in the range $0.5 < P_T < 1.5$ GeV$/c$. It should be noted that this asymmetry was measured at HERA by ZEUS, but at very low x and very high Q^2 [35], where other QCD effects dominate. It was also measured at CERN by EMC [74], but with low precision. Those data were approximated by Barone, Lu, and Ma [75] in a u-quark dominating model for $h_1^\perp$, with a Gaussian, algebraic form and a Gaussian ansatz for the Collins function. Our dynamical approach leads to different predictions for the forthcoming JLab data.

B. Single-spin asymmetry $A_{UL}^{\sin(2\phi)}$ in SIDIS

Since we have calculated the chiral-odd but T-even parton distribution $h_{1L}^\perp$ [cf. Eqs (12) and (13)], we use this result together with the result of Ref. [71] for the Collins function to give a prediction for the $\sin(2\phi)$ moment of the single-spin asymmetry A_{UL} for a longitudinally polarized target. In particular, we are able to take into account the flavor dependence of the asymmetry. We adopt a similar procedure for the azimuthal $\cos(2\phi)$ asymmetry for treating the leading twist observable $A_{UL}^{\sin(2\phi)}$.

A decomposition into structure functions of the cross section of semi-inclusive DIS for a longitudinally polarized target reads (see e.g. [31])

$$\frac{d\sigma_{UL}}{dxdydzd\phi_h dP_{h\perp}^2} \approx \frac{2\pi\alpha^2}{xyQ^2} S_\parallel [(1-y)\sin(2\phi_h) F_{UL}^{\sin(2\phi)} + (2-y)\sqrt{1-y}\sin(\phi_h) F_{UL}^{\sin\phi}], \tag{46}$$

where $S_\parallel$ is the projection of the spin vector on the direction of the virtual photon. In a partonic picture the structure function $F_{UL}^{\sin(2\phi)}$ is a leading twist object (while $F_{UL}^{\sin\phi}$ is subleading), and it is given by a convolution of the TMD $h_{1L}^\perp$ and the Collins function (cf. [31])

$$F_{UL}^{\sin(2\phi)} = \mathcal{C}\left[-\frac{2\hat{\boldsymbol{h}}\cdot\boldsymbol{k}_T \hat{\boldsymbol{h}}\cdot\boldsymbol{p}_T - \boldsymbol{k}_T\cdot\boldsymbol{p}_T}{MM_h} h_{1L}^\perp H_1^\perp \right], \tag{47}$$

where the explicit form of the convolution is given in Eq. (42).

We insert our result for $h_{1L}^\perp$ [Eqs. (12) and (13)] and the result of Ref. [71] into Eq. (47) to compute the single-spin asymmetry. This is the first calculation of this observable in the spectator framework, whereas the part of $F_{UL}^{\sin(\phi)}$ described by higher twist T-odd PDFs has been analyzed in the diquark model in Refs. [25,26,28]. Similar phenomenology for $F_{UL}^{\sin(2\phi)}$ and $F_{UL}^{\sin(\phi)}$ has been performed in Refs. [76,77] using the framework of the chiral quark soliton model.

We display the results for the single-spin asymmetry $A_{UL}^{\sin(2\phi)}$ in Fig. 8 using the kinematics of the upcoming

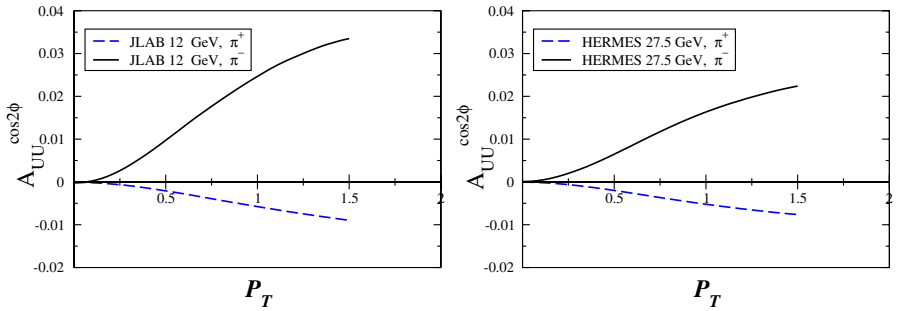

FIG. 6 (color online). Left panel: The $\cos 2\phi$ asymmetry for π^+ and π^- as a function of P_T at JLab 12 GeV kinematics. Right panel: The $\cos 2\phi$ asymmetry for π^+ and π^- as a function of P_T for HERMES kinematics.

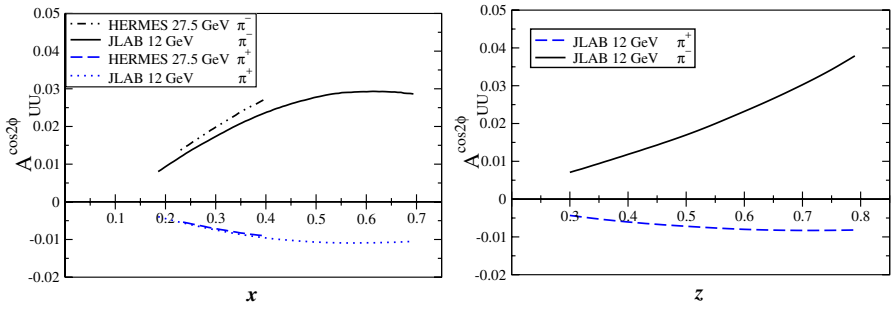

FIG. 7 (color online). Left panel: The $\cos 2\phi$ asymmetry for π^+ and π^- as a function of x at JLab 12 GeV and HERMES kinematics. Right panel: The $\cos 2\phi$ asymmetry for π^+ and π^- as a function of z for JLab kinematics.

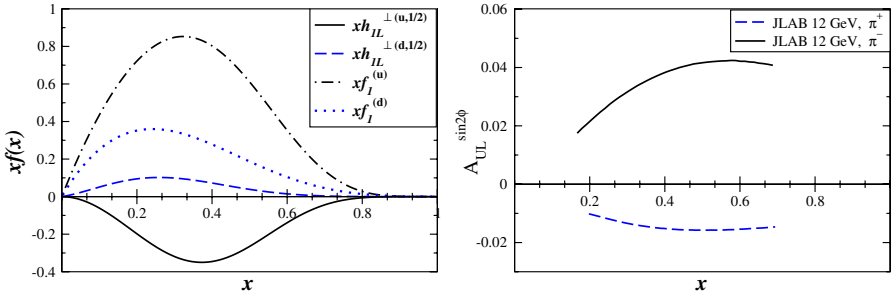

FIG. 8 (color online). Left panel: The half-moment of $xh_{1L}^{\perp(1/2)}$ versus x compared to the unpolarized u- and d-quark distribution functions. Right panel: The $\sin 2\phi$ asymmetry for π^+ and π^- as a function of x at JLab 12 GeV kinematics.

JLab 12 GeV upgrade. We note that the π^- asymmetry is large and positive due to the model assumption $H_1^{\perp(\mathrm{dis-fav})} \approx -H_1^{\perp(\mathrm{fav})}$. This asymmetry has been measured at HERMES for longitudinally polarized protons [19] and deuterons [21]. The data show that for the proton target and HERMES 27.5 GeV kinematics both π^+ and π^- asymmetries are consistent with 0 down to a sensitivity of about 0.01. That is to say, these asymmetries could be nonzero, but with magnitudes less than 0.01 or 0.02. These results are considerably smaller than our predictions for the JLab upgrade. For the deuteron target the results are consistent with 0 for π^+ and π^-. There is one π^0 point at $x \sim 0.2$ that could be positive at about 0.03. This SIDIS data for polarized deuterons could reflect the near cancellation of u- and d-quark $h_{1L}^{\perp}$ functions and/or the large unfavored Collins function contributions. There are also CLAS preliminary data [78] at 5.7 GeV that show slightly negative asymmetries for π^+ and π^- and lead to the extraction of a negative $xh_{1L}^{\perp(u)}$. This suggests that the unfavored Collins function (for $d \to \pi^+$) is not contributing much here, unlike the inference from the HERMES data. Data from the upgrade should help resolve these phenomenological questions.

V. CONCLUSIONS

In this paper we performed calculations of transverse-momentum-dependent parton distributions, including the Boer-Mulders function $h_1^{\perp}$, the Sivers function $f_{1T}^{\perp}$, and $h_{1L}^{\perp}$ in the diquark spectator model, taking into account both axial-vector and scalar contributions. The calculation of these functions in both sectors allowed us to explore their flavor dependence, i.e. to compute their u-quark and d-quark contributions. For T-even distributions like $h_{1L}^{\perp}$, a nontrivial contribution could already have been obtained from a tree-level diagram. By contrast, final state interactions or, equivalently, contributions from the gauge link had to be taken into account for the T-odd Boer-Mulders and Sivers functions, requiring the calculation of a loop (box) diagram. It was found that the loop integrals for $f_{1T}^{\perp}$ and $h_1^{\perp}$ show light-cone divergences and UV divergences in the axial-vector diquark sector, in contrast to the scalar diquark sector. We regularized these divergences by choosing specific types of the phenomenologically motivated nucleon-diquark-quark form factors. By comparing the model expression for the unpolarized parton distribution, f_1, with the low-scale parametrizations of that function obtained from data, it is possible to fix most of the parameters of the model, masses, normalization and R_g, the ratio of axial diquark couplings to the nucleon. In order to fix the sign and size of the final state interactions specific for T-odd distributions, we calculated the Sivers function and compared the result to parametrizations of SIDIS data already determined in a global fit for $f_{1T}^{\perp}$. In such a way, the remaining parameters could be fixed, and predictions were presented for the flavor dependence of the Boer-Mulders function $h_1^{\perp}$ for a u quark and a d quark. We find that the k_T half and first moments of

this function are negative for both flavors. This result is in contrast to that in [41]. Our sign result is in agreement with other approaches that predict negative $h_1^{\perp(u)}$ and $h_1^{\perp(d)}$.

We also note that the resulting u-quark Sivers function and Boer-Mulders function are nearly equal, even with the inclusion of the axial-vector spectator diquark. This near equality $h_1^\perp \sim f_{1T}^\perp$ was obtained from models without axial diquarks, hinting at some more general mechanism that preserves the relation.

We used our result for $h_1^\perp$ as one ingredient in the factorized formula for the azimuthal asymmetry $A_{UU}^{(\cos(2\phi))}$ in unpolarized semi-inclusive lepto-production of positively and negatively charged pions. We also used our $h_{1L}^\perp$ as an ingredient in the single-spin asymmetry $A_{UL}^{(\sin(2\phi))}$ for a longitudinally polarized target in semi-inclusive DIS. Another key ingredient for determining such asymmetries is the Collins fragmentation function $H_1^\perp$. For this function we used the most current expressions that were obtained in a similar spectator model.

We provide estimates for $A_{UU}^{(\cos(2\phi))}$ and $A_{UL}^{(\sin(2\phi))}$. The latter has already been measured at HERMES and preliminarily by CLAS. There are important differences in the kinematic regions explored, but there remain discrepancies that may be resolved in the future at Jefferson Lab, for which our model gives striking predictions of relatively large asymmetries. The nontrivial π^- asymmetry is driven in large part by the model assumption $H_1^{\perp(\text{dis}-\text{fav})} \approx -H_1^{\perp(\text{fav})}$ in the pion sector. We note that our result for $A_{UL}^{(\sin(2\phi))}$ is the first phenomenological treatment in the spectator framework of this observable.

The former unpolarized asymmetry, $A_{UU}^{(\cos(2\phi))}$, was measured at HERA, but for very small x and extremely high Q^2. Again, this will be measured in the future at JLab. We predict that those results should correspond to the opposite sign asymmetries for opposite charged pions.

In summary, a refined diquark spectator model, including axial-vector diquarks, leads to both u- and d-quark T-odd TMDs and provides the ingredients for predicting a range of asymmetries for future experiments. The approach we have been taking is to use and refine a model for the soft regime that makes sense in QCD and can be applied broadly to a range of measurable phenomena. We have fixed the parameters in the model to approach the inferred structure of the lowest order asymmetries. Combined with the recent determination of the fragmentation functions, we have predicted new SIDIS results. The spirit of this work is to understand the dynamics of processes like SIDIS by refining a robust and flexible model for the T-odd functions that compares with existing data. While a global fit to all the data eventually can be performed, the underlying mechanism is likely to be revealed by honing in on more sophisticated and inclusive models, as we have done here.

ACKNOWLEDGMENTS

We thank Alessandro Bacchetta and Asmita Mukherjee for fruitful discussions and use of results from [71]. This work is supported in part by the U.S. Department of Energy under Contracts No. DE-FG02-07ER41460 (L. G.) and No. DE-FG02-92ER40702 (G. R. G.). Authored by Jefferson Science Associates, LLC under U.S. DOE Contract No. DE-AC05-06OR23177.

APPENDIX A: AXIAL DIQUARK CONTRIBUTION TO THE BOER-MULDERS FUNCTION

The coefficients appearing in the calculation of the Boer-Mulders function for the axial-vector diquark (see text) read

$$A_p = (1-x)[(2Mm_q + (2-R_g)M^2 + R_g m_q^2)(3+2\kappa) + R_g m_s^2(7+4\kappa)], \tag{A1}$$

$$B_p = (1-x)[(2Mm_q + (2-R_g)M^2 + R_g m_q^2)(3+2\kappa) + R_g m_s^2(11+6\kappa)], \tag{A2}$$

$$\begin{aligned} C_p = {} & 2m_s^2(1-x)[2Mm_q(-1+2x(2+\kappa)) \\ & + R_g(m_s^2 + 6\vec{p}_T^{\,2}(2+\kappa) + m_q^2(3+2\kappa)) \\ & + M^2(-2+4x(2+\kappa) \\ & + R_g(1-2x(2-x)(2+\kappa)))], \end{aligned} \tag{A3}$$

$$\begin{aligned} D_p = {} & 2m_s^2(1-x)[2Mm_q(-1+2x(2+\kappa)) \\ & + R_g(m_s^2 + 2\vec{p}_T^{\,2}(2+\kappa) + m_q^2(3+2\kappa)) \\ & + M^2(-2+4x(2+\kappa) \\ & + R_g(1-2x(2-x)(2+\kappa)))], \end{aligned} \tag{A4}$$

$$E_p = 0, \tag{A5}$$

$$\begin{aligned} A_l = {} & -\frac{R_g(3+2\kappa)}{2M}[R_g m_q(m_s^2 - \vec{p}_T^{\,2}) \\ & + M^2 m_q(2-R_g)(1-x)^2 + x(1-x)^2 R_g M^3 \\ & + M((2-R_g)xm_s^2 - \vec{p}_T^{\,2}(2-xR_g))], \end{aligned} \tag{A6}$$

$$\begin{aligned} B_l = {} & -\frac{R_g}{2M}\Big[(3+2\kappa)\Big[M^2 m_q(2-R_g)(1-x)^2 \\ & + x(1-x)^2 R_g M^3 + m_q R_g\Big(-\vec{p}_T^{\,2} + m_s^2\frac{7+4\kappa}{3+2\kappa}\Big)\Big] \\ & + M[-\vec{p}_T^{\,2}(2-xR_g)(3+2\kappa) + m_s^2(4(2+\kappa) \\ & + x(6-7R_g+4\kappa(1-R_g)))]\Big], \end{aligned} \tag{A7}$$

$$C_l = -\frac{1}{2M}[(1-x)^3(3+2\kappa)M^4 m_q(-4+(4-R_g)(1-x)R_g) - (1-x)^3 x(3+2\kappa)M^5 R_g(2-(1-x)R_g) + m_q R_g^2(8m_s^2\vec{p}_T^{\,2}(2+\kappa) + (m_s^2-\vec{p}_T^{\,2})(m_s^2+\vec{p}_T^{\,2})(3+2\kappa)) + MR_g(xm_s^4(2-R_g)(3+2\kappa) - \vec{p}_T^{\,4}(2-xR_g)(3+2\kappa) - 2m_s^2\vec{p}_T^{\,2}(-17+x+8xR_g-8\kappa+4xR_g\kappa) + 2m_q^2(1-x)(m_s^2+(3+2\kappa)\vec{p}_T^{\,2})) + 2(1-x)M^2 m_q(\vec{p}_T^{\,2}(3+2\kappa)(2+(1-x)R_g(2-R_g)) + m_s^2(4(2+\kappa)-x(6+4\kappa))) + 2(1-x)M^3(-m_q^2(2-R_g)(1-x)^2(3+2\kappa) + \vec{p}_T^{\,2}(2-R_g+x(1-x)R_g^2)(3+2\kappa) + xm_s^2(2+R_g(6-7x+4\kappa(1-x))))], \tag{A8}$$

$$D_l = \frac{m_s^2}{M}[-m_q R_g^2(m_s^2+\vec{p}_T^{\,2}) + (1-x)^2M^2 m_q R_g(2-R_g) + M^3(1-x)^2(xR_g^2+4(2+\kappa)-2R_g(1+x)(2+\kappa)) + MR_g(m_s^2(2\kappa-x(2-R_g+2\kappa)) + \vec{p}_T^{\,2}(x(4+R_g+2\kappa)-2(3+\kappa)))], \tag{A9}$$

$$E_l = \frac{m_s^2}{M}[-m_q R_g^2(\vec{p}_T^{\,2}+m_s^2)^2 + M^4 m_q(1-x)^3(-4+(1-x)(4-R_g)R_g + 8x(2+\kappa)) - x(1-x)^3M^5R_g(2-(1-x)R_g - 4x(2+\kappa)) - 2M^2 m_q(1-x)(m_s^2(4+(1-x)(2-R_g)R_g - 2x(3+2\kappa)) + \vec{p}_T^{\,2}(-2-(1-x)(2-R_g)R_g) + 4x(2+\kappa))) + MR_g(-x(2-R_g)m_s^4 + 2m_s^2\vec{p}_T^{\,2}(2\kappa-1-x(1-R_g+2\kappa)) + 2m_q^2(1-x)(m_s^2(1+2\kappa) - \vec{p}_T^{\,2}(3+2\kappa)) + \vec{p}_T^{\,4}(x(8+R_g+4\kappa)-2(5+2\kappa))) - 2(1-x)M^3(-m_q^2(1-x)^2(2-R_g)(3+2\kappa) + xm_s^2(6-8x+R_g(-2+R_g+3x-xR_g)-2x\kappa(2-R_g)) + \vec{p}_T^{\,2}(-x(1-x)R_g^2 + R_g(5+2\kappa-4x(2+\kappa)) + 2(-5-2\kappa+4x(2+\kappa))))], \tag{A10}$$

$$A_{lp} = B_{lp} = -4R_g m_s^2(1-x)(2+\kappa), \tag{A11}$$

$$E_{lp} = 4(1-x)m_s^2(2Mm_q(1-x)(2+\kappa) + M^2(1-x)(2-R_g(1-x))(2+\kappa) + R_g(\kappa m_s^2 - \vec{p}_T^{\,2}(2+\kappa))). \tag{A12}$$

APPENDIX B: AXIAL DIQUARK CONTRIBUTION TO THE SIVERS FUNCTION

For the Sivers function the corresponding coefficients read

$$A_p^{\mathrm{Siv}} = -(1-x)(3+2\kappa)\Big(2Mm_q + (2-R_g)M^2 + R_g m_q^2 + R_g m_s^2\frac{7+4\kappa}{3+2\kappa}\Big), \tag{B1}$$

$$B_p^{\mathrm{Siv}} = -(1-x)(3+2\kappa)\Big(2Mm_q + (2-R_g)M^2 + R_g m_q^2 + R_g m_s^2\frac{11+6\kappa}{3+2\kappa}\Big), \tag{B2}$$

$$C_p^{\mathrm{Siv}} = -2(1-x)m_s^2[2Mm_q(-1+2x(2+\kappa)) + R_g(m_s^2+6\vec{p}_T^{\,2}(2+\kappa)+m_q^2(3+2\kappa)) + M^2(-2+4x(2+\kappa) + R_g(1-2x(2-x)(2+\kappa)))], \tag{B3}$$

$$D_p^{\mathrm{Siv}} = -2(1-x)m_s^2[2Mm_q(-1+2x(2+\kappa)) + R_g(m_s^2+2\vec{p}_T^{\,2}(2+\kappa)+m_q^2(3+2\kappa)) + M^2(-2+4x(2+\kappa) + R_g(1-2x(2-x)(2+\kappa)))], \tag{B4}$$

$$E_p^{\mathrm{Siv}} = 0, \tag{B5}$$

$$A_l^{\mathrm{Siv}} = \frac{3+2\kappa}{2M}R_g[R_g m_q(m_s^2-\vec{p}_T^{\,2}) + M^2 m_q(2-R_g)(1-x)^2 + x(1-x)^2R_g M^3 + M(xm_s^2(2-R_g) - \vec{p}_T^{\,2}(2-xR_g))], \tag{B6}$$

$$B_l^{\mathrm{Siv}} = \frac{R_g}{2M}\Big[(3+2\kappa)(M^2 m_q(2-R_g)(1-x)^2 + M^3R_g x(1-x)^2 + m_q R_g\Big(-\vec{p}_T^{\,2} + m_s^2\frac{7+4\kappa}{3+2\kappa}\Big) - M\vec{p}_T^{\,2}(2-xR_g)) + Mm_s^2(4(2+\kappa) + x(6-7R_g+4\kappa(1-R_g)))\Big], \tag{B7}$$

$$C_l^{\mathrm{Siv}} = \frac{1}{2M}[-(1-x)^3M^4m_q(4-(4-R_g)R_g(1-x))(3+2\kappa) - x(1-x)^3M^5R_g(2-(1-x)R_g)(3+2\kappa)$$
$$+ m_qR_g^2(8m_s^2\vec{p}_T^{\,2}(2+\kappa) + (m_s^2-\vec{p}_T^{\,2})(m_s^2+\vec{p}_T^{\,2})(3+2\kappa)) + MR_g(xm_s^4(2-R_g)(3+2\kappa)$$
$$- \vec{p}_T^{\,4}(2-xR_g)(3+2\kappa) + 2m_s^2\vec{p}_T^{\,2}(17-x-8xR_g+8\kappa-4xR_g\kappa) + 2m_q^2(1-x)(m_s^2+\vec{p}_T^{\,2}(3+2\kappa)))$$
$$- 2M^2m_q(1-x)(-\vec{p}_T^{\,2}(2+(2-R_g)R_g(1-x))(3+2\kappa) - m_s^2(4(2+\kappa)-x(6+4\kappa)))$$
$$+ 2M^3(1-x)(-m_q^2(2-R_g)(1-x)^2(3+2\kappa) + \vec{p}_T^{\,2}(2-R_g+x(1-x)R_g^2)(3+2\kappa)$$
$$+ xm_s^2(2+R_g(6-7x+4\kappa(1-x))))], \tag{B8}$$

$$D_l^{\mathrm{Siv}} = -\frac{m_s^2}{M}[-m_qR_g^2(m_s^2+\vec{p}_T^{\,2}) + m_qM^2(1-x)^2R_g(2-R_g) + (1-x)^2M^3(xR_g^2+4(2+\kappa)-2R_g(1+x)(2+\kappa))$$
$$+ MR_g(m_s^2(x(-2+R_g-2\kappa)+2\kappa) + \vec{p}_T^{\,2}(-2(3+\kappa)+x(4+R_g+2\kappa)))], \tag{B9}$$

$$E_l^{\mathrm{Siv}} = -\frac{m_s^2}{M}[-m_q(m_s^2+\vec{p}_T^{\,2})^2R_g^2 + M^4m_q(1-x)^3(-4+(4-R_g)R_g(1-x)+8x(2+\kappa))$$
$$- M^5R_gx(1-x)^3(2-(1-x)R_g-4x(2+\kappa)) + 2M^2m_q(1-x)(\vec{p}_T^{\,2}(2+(2-R_g)R_g(1-x)-4x(2+\kappa))$$
$$+ m_s^2(2x+4x\kappa-(2-R_g)R_g(1-x))) + MR_r(-xm_s^4(2-R_g) + 2m_s^2\vec{p}_T^{\,2}(2\kappa-1-x(1-R_g+2\kappa))$$
$$+ 2m_q^2(1-x)(m_s^2(1+2\kappa) - \vec{p}_T^{\,2}(3+2\kappa)) + \vec{p}_T^{\,4}(-2(5+2\kappa)+x(8+R_g+4\kappa)))$$
$$- 2M^3(1-x)(-m_q^2(2-R_g)(1-x)^2(3+2\kappa) + xm_s^2(2-4x-R_g(2-R_g-3x+xR_g)$$
$$- 2(2-R_g)x\kappa) + \vec{p}_T^{\,2}(-x(1-x)R_g^2 + R_g(5+2\kappa-4x(2+\kappa)) - 2(5+2\kappa-4x(2+\kappa)))], \tag{B10}$$

$$A_{lk}^{\mathrm{Siv}} = B_{lk}^{\mathrm{Siv}} = E_{lk}^{\mathrm{Siv}} = 0. \tag{B11}$$

APPENDIX C: $\mathcal{R}$ FUNCTIONS

The $\mathcal{R}$ functions appearing in the text are defined in the following. The $\mathcal{R}$ function for the unpolarized PDF f_1 for an axial-vector diquark reads

$$\mathcal{R}_1^{ax}(x, \vec{p}_T^{\,2}; R_g, \{\mathcal{M}\}) \tag{C1}$$

$$= M^2[(\vec{p}_T^{\,2})^2 + 2(1-x(1-x))m_s^2\vec{p}_T^{\,2} + x^2m_s^4 + 6x(1-x)^2m_qMm_s^2 + (1-x)^2M^2(\vec{p}_T^{\,2}+2x^2m_s^2+(1-x)^2m_q^2)$$
$$+ m_q^2(1-x)^2(\vec{p}_T^{\,2}+2m_s^2)] + R_g[M^2(-(\vec{p}_T^{\,2})^2 - x^2m_s^4 + (1-(4-x)x)m_s^2\vec{p}_T^{\,2} - (1-x)^2m_q^2(\vec{p}_T^{\,2}-m_s^2)$$
$$- M^2(1-x)^2(\vec{p}_T^{\,2} - x^2m_s^2 + (1-x)^2m_q^2) + m_qM(x(\vec{p}_T^{\,2}+m_s^2)^2 + 2x(1-x)^2M^2(\vec{p}_T^{\,2}-m_s^2+x(1-x)^4M^2))]$$
$$+ R_g^2\left[\frac{1}{4}(\vec{p}_T^{\,2} + (m_s-(1-x)M)^2)(\vec{p}_T^{\,2} + (xM-m_q)^2)(\vec{p}_T^{\,2} + (m_s+(1-x)M)^2)\right]. \tag{C2}$$

The corresponding $\mathcal{R}$ function for $h_{1L}^{\perp,ax}$ reads

$$\mathcal{R}_{1L}^{\perp,ax}(x, \vec{p}_T^{\,2}; R_g, \{\mathcal{M}\}) \tag{C3}$$

$$= -m_qR_g^2(m_s^2+\vec{p}_T^{\,2})^2 + 2m_qM^2(1-x)(\vec{p}_T^{\,2}[2+R_g(1-x)(2-R_g) + m_s^2[2(2-x) - R_g(1-x)(2-R_g)])$$
$$- M^4m_q(1-x)^3[4-(4-R_g)R_g(1-x)] - x(1-x)^3M^5R_g(2-(1-x)R_g) + MR_g(m_s^2+\vec{p}_T^{\,2})[2(1-x)m_q^2$$
$$- xm_s^2(2-R_g) - \vec{p}_T^{\,2}(2-xR_g)] + 2(1-x)M^3(-m_q^2(1-x)^2(2-R_g) + xm_s^2(2+R_g(2-(1-x)R_g-3x))$$
$$+ \vec{p}_T^{\,2}(2-R_g+x(1-x)R_g^2). \tag{C4}$$

The $\mathcal{R}$ function for the T-odd functions $h_1^{\perp}$ and $f_{1T}^{\perp}$ is more complicated and contains incomplete Gamma functions (see text) with $a \equiv \tilde{b}\tilde{m}_\Lambda^2$, $c \equiv \tilde{b}(\vec{p}_T^{\,2} + \tilde{m}_\Lambda^2)$, $d \equiv \tilde{b}\vec{p}_T^{\,2}$,

$$\mathcal{R}_1^{\perp,ax}(x, \vec{p}_T^{\,2}; R_g, \kappa, \tilde{b}, \Lambda, \{\mathcal{M}\}) \tag{C5}$$

$$\begin{aligned}
&= \mathcal{R}_{1T}^{\perp,ax}(x, \vec{p}_T^{\,2}; R_g, \kappa, \tilde{b}, \Lambda, \{\mathcal{M}\}) \\
&= (A_p - 2A_l + B_l)\left[-\tilde{b}\mathrm{e}^a\left(1+\frac{a}{2}\right)\Gamma(0,a) + \frac{\tilde{b}}{2}\frac{1+a}{a}\right] + (\vec{p}_T^{\,2}[A_p - A_l - 2(B_p - B_l)] + C_p - C_l)\left[\frac{\tilde{b}^2}{2}\mathrm{e}^a\Gamma(0,a)\right. \\
&\quad \left. + \tilde{b}^2\frac{1-a}{2a^2}\right] + \frac{A_{lp}}{2\vec{p}_T^{\,2}}\left[\left(1+2a+\frac{a^2}{2}\right)\mathrm{e}^a(\Gamma(0,a)-\Gamma(0,c)) - \frac{3+a}{2} - \mathrm{e}^{-d}\frac{a^2(1-c)-4ac}{2c^2}\right] \\
&\quad + \left(-\frac{A_{lp}}{2} - \frac{D_l}{\vec{p}_T^{\,2}} + \frac{E_{lp}}{2\vec{p}_T^{\,2}}\right)\left[-\tilde{b}\mathrm{e}^a\left(1+\frac{a}{2}\right)(\Gamma(0,a)-\Gamma(0,c)) + \frac{\tilde{b}}{2}\frac{1+a}{a} - \frac{\tilde{b}}{2c^2}\mathrm{e}^{-d}(2c-a(1-c))\right] \\
&\quad + \left(-2(D_p - D_l) - \frac{E_l}{\vec{p}_T^{\,2}}\right)\left[\frac{\tilde{b}^2}{2}\mathrm{e}^a(\Gamma(0,a)-\Gamma(0,c)) + \tilde{b}^2\frac{1-a}{2a^2} - \tilde{b}^2\frac{1-c}{2c^2}\mathrm{e}^{-d}\right] + \frac{A_{lp}}{2}\left[-\tilde{b}\mathrm{e}^a\left(1+\frac{a}{2}\right)\Gamma(0,c)\right. \\
&\quad \left. + \frac{\tilde{b}}{2c^2}(2c-a(1-c))\mathrm{e}^{-d}\right] + \left(-\vec{p}_T^{\,2}\frac{A_{lp}}{2} + D_l + \frac{1}{2}E_{lp}\right)\left[\frac{\tilde{b}^2}{2}\mathrm{e}^a\Gamma(0,c) + \tilde{b}^2\frac{1-c}{2c^2}\mathrm{e}^{-d}\right].
\end{aligned} \tag{C6}$$

[1] A. Airapetian *et al.* (HERMES), Phys. Rev. Lett. **94**, 012002 (2005).
[2] V. Y. Alexakhin *et al.* (COMPASS), Phys. Rev. Lett. **94**, 202002 (2005).
[3] L. Y. Zhu *et al.* (FNAL-E866/NuSea), Phys. Rev. Lett. **99**, 082301 (2007).
[4] V. Barone *et al.* (PAX), arXiv:hep-ex/0505054.
[5] A. Afanasev *et al.*, arXiv:hep-ph/0703288.
[6] D. W. Sivers, Phys. Rev. D **41**, 83 (1990).
[7] D. W. Sivers, Phys. Rev. D **43**, 261 (1991).
[8] D. Boer and P. J. Mulders, Phys. Rev. D **57**, 5780 (1998).
[9] J. C. Collins, Phys. Lett. B **536**, 43 (2002).
[10] A. V. Belitsky, X. Ji, and F. Yuan, Nucl. Phys. **B656**, 165 (2003).
[11] D. Boer, P. J. Mulders, and F. Pijlman, Nucl. Phys. **B667**, 201 (2003).
[12] S. J. Brodsky, D. S. Hwang, and I. Schmidt, Phys. Lett. B **530**, 99 (2002).
[13] D. Boer, S. J. Brodsky, and D. S. Hwang, Phys. Rev. D **67**, 054003 (2003).
[14] X.-d. Ji and F. Yuan, Phys. Lett. B **543**, 66 (2002).
[15] P. J. Mulders and R. D. Tangerman, Nucl. Phys. **B461**, 197 (1996).
[16] X.-d. Ji, J.-p. Ma, and F. Yuan, Phys. Rev. D **71**, 034005 (2005).
[17] X.-d. Ji, J.-P. Ma, and F. Yuan, Phys. Lett. B **597**, 299 (2004).
[18] J. C. Collins and A. Metz, Phys. Rev. Lett. **93**, 252001 (2004).
[19] A. Airapetian *et al.* (HERMES), Phys. Rev. Lett. **84**, 4047 (2000).
[20] A. Airapetian *et al.* (HERMES), Phys. Rev. D **64**, 097101 (2001).
[21] A. Airapetian *et al.* (HERMES), Phys. Lett. B **562**, 182 (2003).
[22] A. Airapetian *et al.* (HERMES), Phys. Lett. B **622**, 14 (2005).
[23] H. Avakian *et al.* (CLAS), Phys. Rev. D **69**, 112004 (2004).
[24] A. Airapetian *et al.* (HERMES), Phys. Lett. B **648**, 164 (2007).
[25] A. Afanasev and C. E. Carlson, arXiv:hep-ph/0308163.
[26] A. Metz and M. Schlegel, Eur. Phys. J. A **22**, 489 (2004).
[27] A. Metz and M. Schlegel, Ann. Phys. (Leipzig) **13**, 699 (2004).
[28] A. V. Afanasev and C. E. Carlson, Phys. Rev. D **74**, 114027 (2006).
[29] A. Bacchetta, P. J. Mulders, and F. Pijlman, Phys. Lett. B **595**, 309 (2004).
[30] K. Goeke, A. Metz, and M. Schlegel, Phys. Lett. B **618**, 90 (2005).
[31] A. Bacchetta *et al.*, J. High Energy Phys. 02 (2007) 093.
[32] J. C. Collins, Nucl. Phys. **B396**, 161 (1993).
[33] D. Boer, Phys. Rev. D **60**, 014012 (1999).
[34] J. Breitweg *et al.* (ZEUS), Phys. Lett. B **481**, 199 (2000).
[35] S. Chekanov *et al.* (ZEUS), Eur. Phys. J. C **51**, 289 (2007).
[36] S. Falciano *et al.* (NA10), Z. Phys. C **31**, 513 (1986).
[37] M. Guanziroli *et al.* (NA10), Z. Phys. C **37**, 545 (1988).
[38] J. S. Conway *et al.*, Phys. Rev. D **39**, 92 (1989).
[39] Z. Lu, B.-Q. Ma, and I. Schmidt, Phys. Lett. B **639**, 494 (2006).
[40] F. Yuan, Phys. Lett. B **575**, 45 (2003).
[41] A. Bacchetta, A. Schäfer, and J.-J. Yang, Phys. Lett. B **578**, 109 (2004).
[42] P. V. Pobylitsa, arXiv:hep-ph/0301236.
[43] B. Pasquini, M. Pincetti, and S. Boffi, Phys. Rev. D **72**, 094029 (2005).
[44] M. Gockeler *et al.* (QCDSF), Phys. Rev. Lett. **98**, 222001 (2007).
[45] M. Burkardt, Phys. Rev. D **72**, 094020 (2005).

[46] M. Burkardt and B. Hannafious, Phys. Lett. B **658**, 130 (2008).
[47] S. Meissner, A. Metz, and K. Goeke, Phys. Rev. D **76**, 034002 (2007).
[48] G. R. Goldstein and L. Gamberg, in *Proceedings of ICHEP 2002*, edited by S. Bentvelsen *et al.* (North Holland, Amsterdam, 2003), p. 452, arXiv:hep-ph/0209085.
[49] L. P. Gamberg, G. R. Goldstein, and K. A. Oganessyan, Phys. Rev. D **67**, 071504 (2003).
[50] A. M. Kotzinian and P. J. Mulders, Phys. Lett. B **406**, 373 (1997).
[51] A. Metz, Phys. Lett. B **549**, 139 (2002).
[52] L. P. Gamberg, G. R. Goldstein, and K. A. Oganessyan, Phys. Rev. D **68**, 051501 (2003).
[53] R. Jakob, P. J. Mulders, and J. Rodrigues, Nucl. Phys. **A626**, 937 (1997).
[54] R. Ali and P. Hoodbhoy, Phys. Rev. D **51**, 2302 (1995).
[55] L. P. Gamberg, D. S. Hwang, A. Metz, and M. Schlegel, Phys. Lett. B **639**, 508 (2006).
[56] W. Melnitchouk, A. W. Schreiber, and A. W. Thomas, Phys. Rev. D **49**, 1183 (1994).
[57] G. R. Goldstein and J. Maharana, Nuovo Cimento Soc. Ital. Fis. A **59**, 393 (1980).
[58] M. Jamin and M. E. Lautenbacher, Comput. Phys. Commun. **74**, 265 (1993).
[59] K. Goeke, S. Meissner, A. Metz, and M. Schlegel, Phys. Lett. B **637**, 241 (2006).
[60] R. N. Cahn, Phys. Lett. **78B**, 269 (1978).
[61] E. L. Berger, Phys. Lett. **89B**, 241 (1980).
[62] E. L. Berger, Z. Phys. C **4**, 289 (1980).
[63] H. Georgi and H. D. Politzer, Phys. Rev. Lett. **40**, 3 (1978).
[64] A. Mendez, Nucl. Phys. **B145**, 199 (1978).
[65] M. Glück, E. Reya, and A. Vogt, Eur. Phys. J. C **5**, 461 (1998).
[66] M. Anselmino *et al.*, arXiv:hep-ph/0511017.
[67] M. Anselmino *et al.*, Phys. Rev. D **72**, 094007 (2005).
[68] W. Vogelsang and F. Yuan, Phys. Rev. D **72**, 054028 (2005).
[69] J. C. Collins *et al.*, Phys. Rev. D **73**, 014021 (2006).
[70] J. C. Collins *et al.*, Phys. Rev. D **73**, 094023 (2006).
[71] A. Bacchetta, L. Gamberg, G. Goldstein, and A. Mukherjee, Phys. Lett. B **659**, 234 (2008).
[72] A. Schäfer and O. V. Teryaev, Phys. Rev. D **61**, 077903 (2000).
[73] H. Avakian *et al.*, approved JLab Proposal PR 12-06-112 (2006).
[74] M. Arneodo *et al.* (European Muon), Z. Phys. C **34**, 277 (1987).
[75] V. Barone, Z. Lu, and B.-Q. Ma, Phys. Lett. B **632**, 277 (2006).
[76] A. V. Efremov, K. Goeke, and P. Schweitzer, Phys. Lett. B **522**, 37 (2001).
[77] A. V. Efremov, K. Goeke, and P. Schweitzer, Phys. Rev. D **67**, 114014 (2003).
[78] H. Avakian, P. E. Bosted, V. Burkert, and L. Elouadrhiri (CLAS), AIP Conf. Proc. **792**, 945 (2005).